ELSEVIER

Journal of Alloys and Compounds 434–435 (2007) 221–224

Journal of ALLOYS AND COMPOUNDS

www.elsevier.com/locate/jallcom

Crystallization and thermal stability of the $Mg_{65}Cu_{25-x}Gd_{10}Ag_x$ ($x = 0$–10) amorphous alloys

L.J. Chang [a], J.S.C. Jang [a,*], B.C. Yang [a], J.C. Huang [b]

[a] *Department of Materials Science and Engineering, I-Shou University, Kaohsiung, Taiwan, ROC*
[b] *Institute of Materials Science and Engineering, Center for Nanoscience and Nanotechnology, National Sun Yat-Sen University, Kaohsiung, Taiwan, ROC*

Available online 2 October 2006

Abstract

$Mg_{65}Cu_{25-x}Gd_{10}Ag_x$ ($x = 0$–10) amorphous alloy ribbons with 0.1 mm thickness were prepared by melt spinning. The thermal properties and microstructure development during the annealing of amorphous alloys have been investigated by the combination of differential scanning calorimetry (DSC), SEM with EDS capability, X-ray diffractometry (XRD) and TEM techniques. The XRD result reveals that all these as-quenched $Mg_{65}Cu_{25-x}Gd_{10}Ag_x$ alloy ribbons exhibit broad diffraction patterns of amorphous phase. A clear T_g (glass transition temperature) and supercooled region (about 40 K) were revealed for all $Mg_{65}Cu_{25-x}Gd_{10}Ag_x$ alloy ribbons. In addition, the single stage crystallization of the $Mg_{65}Cu_{25}Gd_{10}$ alloy was found to change into three stage crystallization when the Ag element was added. In parallel, the glass transition temperature for the $Mg_{65}Cu_{25-x}Gd_{10}Ag_x$ alloys exhibits an increasing trend with Ag content. However, the crystallization temperature T_x and supercooled region present a decreasing trend with Ag content.

Keywords: Amorphous; Thermal property; Crystallization

1. Introduction

Magnesium alloys have numerous advantages over steels, cast irons, copper, aluminium alloys and plastics, such as high specific strength/density ratio and high damping capacity [1–3]. However, due to inherent low stiffness and low workability of conventional magnesium alloys, application of magnesium alloys is limited. Therefore, great efforts have been devoted to the development of Mg-based amorphous alloys with high specific strength in bulk form with thickness of over several millimeters for applying as structural materials. The ternary $Mg_{65}Cu_{25}Y_{10}$ alloy was the first to exhibit a good glass forming ability (GFA) so that metallic glass rods with diameters 4 and 7 mm could be fabricated using copper mold casting and high pressure die-casting methods, respectively [4,5]. The critical cooling rate to form the bulk metallic glass (BMG) was estimated about 10^2 K/s. Further improvement of GFA has been reported in the Mg–Cu–Y ternary alloy system where Cu is partially substituted with TM (TM: transition metal such as Ag, Pd, or Zn). For example, $Mg_{65}Cu_{15}Ag_{10}Y_{10}$ [6], $Mg_{65}Cu_{20}Zn_5Y_{10}$ [7], and $Mg_{65}Cu_{15}Ag_5Pd_5Y_{10}$ [8,9] exhibit high GFA and can form metallic glass rods with diameters more than 6 mm by a Cu-mold injection method. More recently, significant improvement of GFA has been reported in Mg–Cu–Gd alloy system [10]. The ternary $Mg_{65}Cu_{25}Gd_{10}$ BMG with diameter of at least 8 mm can be fabricated by conventional Cu-mold casting method in air. In addition, these Mg-based BMGs exhibit high compressive fracture strength up to 850 MPa [11–13], which is about twice as high as the highest strength for conventional Mg-based crystalline alloys.

In this study, the effect of substituting Ag for Cu in $Mg_{65}Cu_{25}Gd_{10}$ alloy on GFA and crystallization behavior was investigated. Selection of Ag as the alloying element was due to following reasons: (1) a large difference in atomic size between Ag and the constituent elements; the atomic radius of Ag is 11% larger than that of Cu and is smaller than those of Mg and Gd by 10% and 19.5%, respectively [14]; (2) Ag and Cu belong to the same family in the periodic table and the number of valence electrons of Ag is the same as for Cu.

2. Experimental procedures

Chemical compositions of alloys for this study were based on $Mg_{65}Cu_{25-x}Gd_{10}Ag_x$, where x varies from 0 to 10. The CuY alloy ingots used in this investigation were pre-alloyed by arc melting in an argon atmosphere.

* Corresponding author.
E-mail addresses: scjang@isu.edu.tw (J.S.C. Jang), jacobc@mail.nsysu.edu.tw (J.C. Huang).

0925-8388/$ – see front matter © 2006 Elsevier B.V. All rights reserved.
doi:10.1016/j.jallcom.2006.08.253

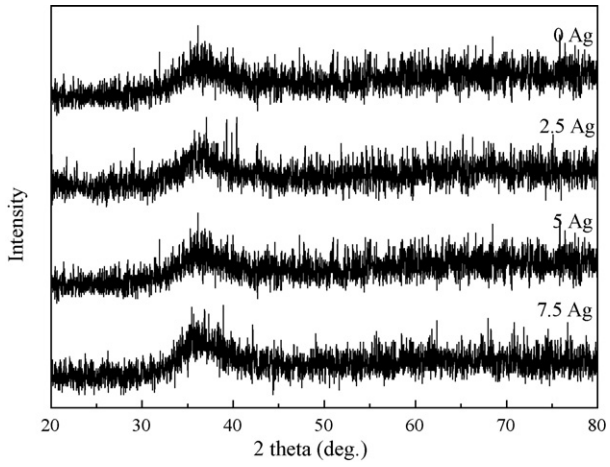

Fig. 1. XRD patterns of as-quenched $Mg_{65}Cu_{25-x}Gd_{10}Ag_x$ amorphous alloys.

The CuY alloy was then melted together with Mg and Ag pieces by induction melting and single roller melt-spinning under argon atmosphere to obtain $Mg_{65}Cu_{25-x}Gd_{10}Ag_x$ ($x = 0$–10) alloy ribbons. The alloy ribbon samples with 0.1 mm in thickness and 5 mm in width. The liquidus temperatures of pre-alloyed samples were determined by Perkin-Elmer DTA 7 differential thermal analyzer (DTA). The thermal properties of the as-quenched samples were determined by TA Instruments DSC 2920 differential scanning calorimeter (DSC). The amorphous ribbons were isothermally annealed for various time at a temperature between glass transition temperature and crystallization temperature. The as-quenched structure and annealed samples were examined by X-ray diffraction (XRD) with monochromatic Cu Kα radiation, transmission electron microscopy (TEM), and nano-beam electron diffraction.

3. Results and discussion

Fig. 1 shows the XRD patterns of the $Mg_{65}Cu_{25-x}Gd_{10}Ag_x$ alloys. No detectable crystalline peak could be resolved and a broad maximum was observed for all as-quenched samples. This observation indicated that complete amorphization of these alloys had been achieved by the single roll melt spinning. In addition, the TEM observation also revealed a uniform amorphous morphology in the as-quenched ribbon for the $Mg_{65}Cu_{22.5}Gd_{10}Ag_{2.5}$ alloy, as shown in Fig. 2.

The liquidus temperatures (T_l) for the $Mg_{65}Cu_{25-x}Gd_{10}Ag_x$ ($x = 0$–10) alloys exhibit a decreasing trend as the Ag content increases, as shows in Fig. 3. The lowest liquidus temperature (about 702 K) occurs at the $Mg_{65}Cu_{15}Gd_{10}Ag_{10}$ alloy. According to the analyses of Turnbull [15], the best metallic glass forming alloys are at or near deep eutectic compositions and result in obtaining highest reduced glass transition temperature T_{rg}. This implies that the alloy $Mg_{65}Cu_{15}Gd_{10}Ag_{10}$ may be the optimum composition for the best GFA in the $Mg_{65}Cu_{25-x}Gd_{10}Ag_x$ alloy system.

In Fig. 4, the results of DSC revealed a clear T_g before crystallization for each amorphous alloy. According to the result of DSC analysis in Fig. 4, the $\Delta T_x = T_x - T_g$ exhibits an increasing trend with increasing Ag content, as shown in Fig. 5. The reduced glass transition temperature T_{rg} (defined as $T_{rg} = T_g/T_l$) and γ value (defined as $\gamma = T_x/T_g + T_l$ [16]) as shown in Figs. 6 and 7 also revealed that the highest γ value (0.407) and a relatively high T_{rg} (0.58) occur for the $Mg_{65}Cu_{22.5}Gd_{10}Ag_{2.5}$ alloy. Compari-

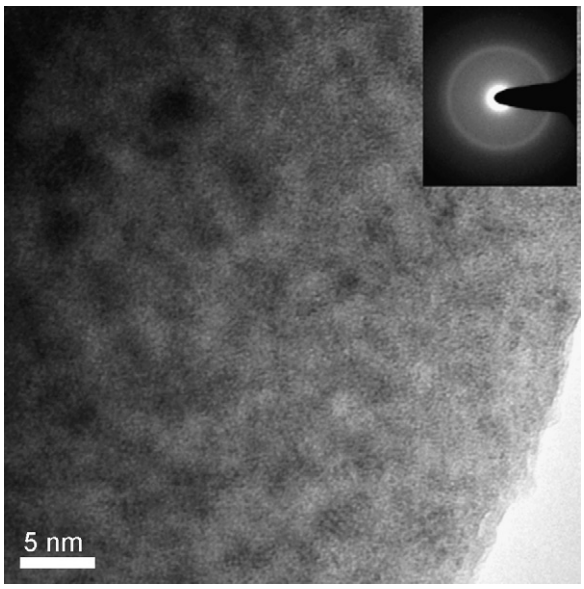

Fig. 2. TEM image of as-quenched $Mg_{65}Cu_{22.5}Gd_{10}Ag_{2.5}$ amorphous alloy.

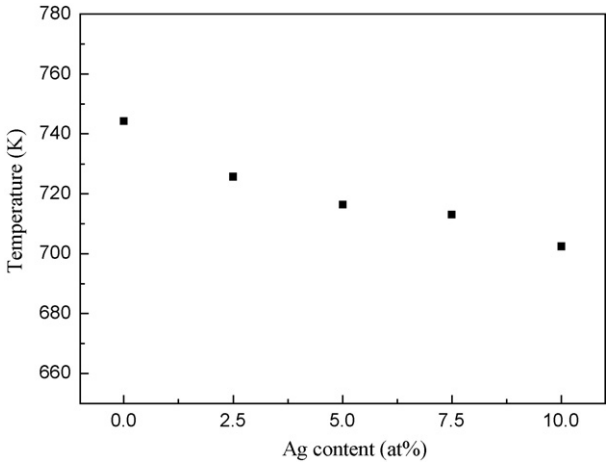

Fig. 3. The variation of liquidus temperature (T_l) with Ag content for $Mg_{65}Cu_{25-x}Gd_{10}Ag_x$ alloys.

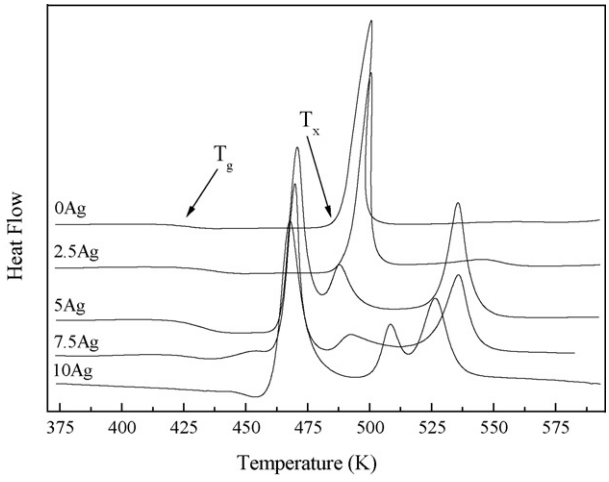

Fig. 4. DSC plots of $Mg_{65}Cu_{25-x}Gd_{10}Ag_x$ amorphous alloy with different Ag content.

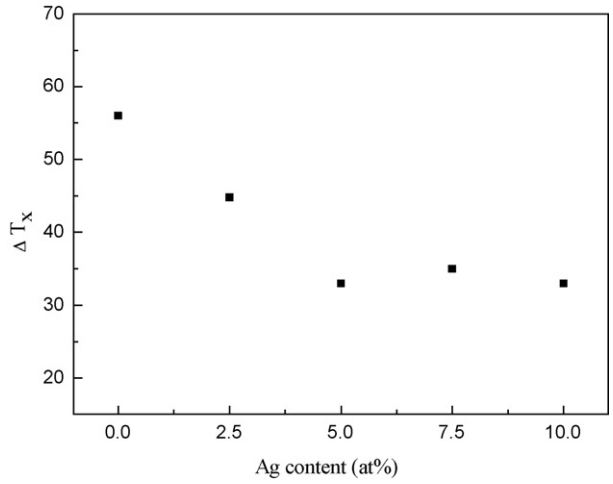

Fig. 5. The ΔT_x of $Mg_{65}Cu_{25-x}Gd_{10}Ag_x$ amorphous alloys as a function of Ag content.

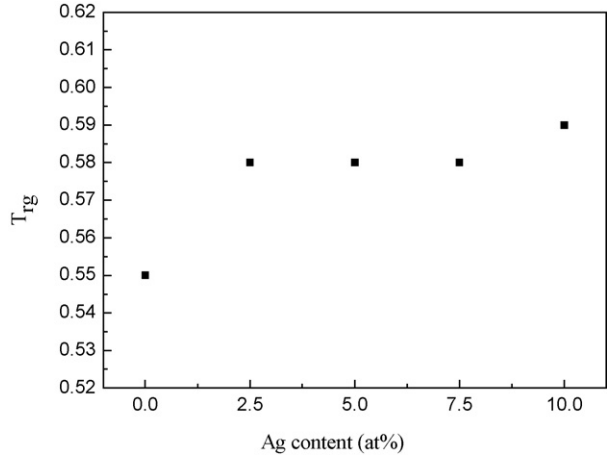

Fig. 6. The variation of T_{rg} value with different Ag content for $Mg_{65}Cu_{25-x}Gd_{10}Ag_x$ amorphous alloy.

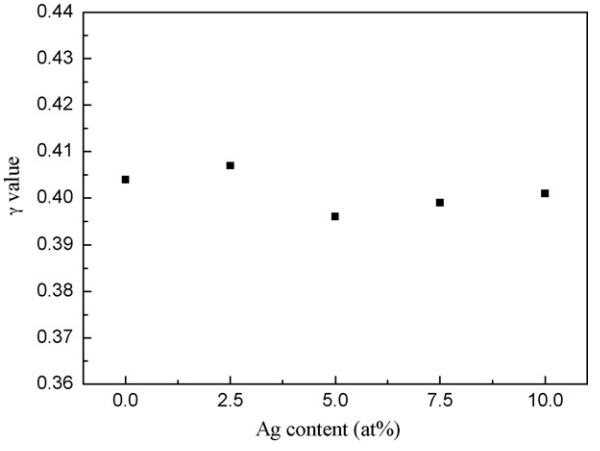

Fig. 7. The variation of γ value with different Ag content for $Mg_{65}Cu_{25-x}Gd_{10}Ag_x$ alloy.

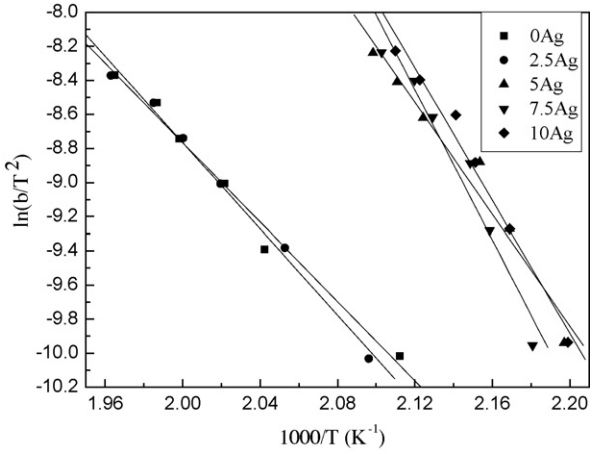

Fig. 8. Kissinger plots of the DSC peaks for crystallization of $Mg_{65}Cu_{25-x}Gd_{10}Ag_x$ alloys.

son of T_{rg} and γ values suggested that the $Mg_{65}Cu_{22.5}Gd_{10}Ag_{2.5}$ alloy would retain a high glass forming ability.

The activation energy for crystallization of the $Mg_{65}Cu_{25-x}Gd_{10}Ag_x$ alloys were determined by the Kissinger plot [17]:

$$\ln\left(\frac{b}{T^2}\right) = -\frac{E_a}{RT} + \text{constant} \quad (1)$$

where b is the heating rate, T_p the crystallization peak temperature, R the gas constant, and E_a is the activation energy. The $\ln(b/T_p^2)$ as a function of $1/T_p$ is plotted in Fig. 8. Fig. 9 shows the activation energy of crystallization calculated by Kissinger plot as a function of silver content for $Mg_{65}Cu_{25-x}Gd_{10}Ag_x$ alloys. The activation energy of $Mg_{65}Cu_{25-x}Gd_{10}Ag_x$ alloys increases with Ag content and reaches the maximum (183 kJ/mol) for the $Mg_{65}Cu_{17.5}Gd_{10}Ag_{7.5}$ alloy. This indicates that the addition of Ag improves the thermal stability for the $Mg_{65}Cu_{25}Gd_{10}$ base alloy.

The kinetic study of crystallization was performed by using the Johnson–Mehl–Avrami (JMA) [18] isothermal analysis for volume fraction x transformed as a function of time t based on

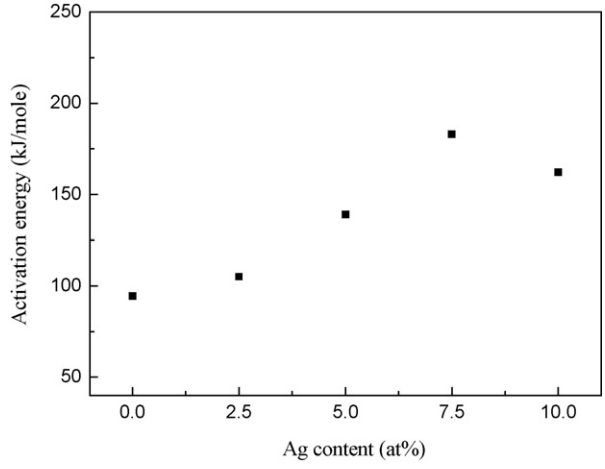

Fig. 9. The activation energy estimated by Kissinger plots as a function of Ag content for $Mg_{65}Cu_{25-x}Gd_{10}Ag_x$ amorphous alloys.

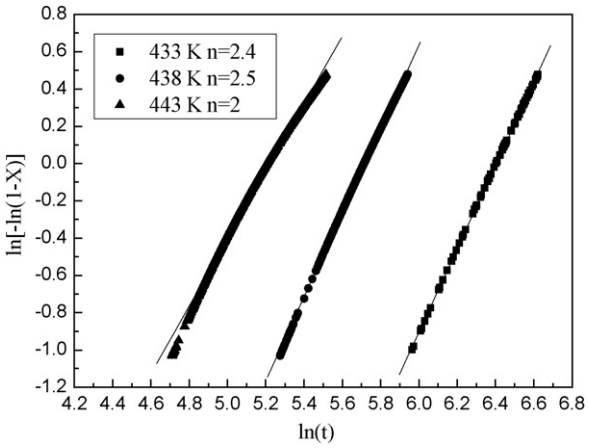

Fig. 10. The JMA plots of $Mg_{65}Cu_{22.5}Gd_{10}Ag_{2.5}$ alloy constructed for $0.1 \leqq X \leqq 0.9$ from the isothermal transformation at several different temperatures.

the following equation [2]:

$$X(t) = 1 - \exp[-(kt)^n] \quad (2)$$

$Mg_{65}Cu_{22.5}Gd_{10}Ag_{2.5}$ were annealed isothermally at several temperatures between T_g and T_x, namely 433, 438, and 443 K. k is an effective rate constant and n is Avrami exponent. The Avrami plots of $\ln[-\ln(1-X)]$ versus $\ln(t)$, constructed for $0.1 \leqq X \leqq 0.9$ at several different temperatures, are shown in Fig. 10. The result reveals that the average value of the Avrami exponent n was 2.3 ± 0.2 for $Mg_{65}Cu_{22.5}Gd_{10}Ag_{2.5}$ alloy. This indicates that $Mg_{65}Cu_{22.5}Gd_{10}Ag_{2.5}$ alloy presents diffusion controlled crystal growth with decreasing nucleation rate [18].

4. Conclusion

According to the results of DTA, DSC, X-ray diffraction, and TEM observation for the $Mg_{65}Cu_{25-x}Gd_{10}Ag_x$ alloys with different Ag content, the effect of Ag on the glass forming abilities and thermal properties can be summarized as:

(1) The liquidus temperatures (T_l) for the $Mg_{65}Cu_{25-x}Gd_{10}Ag_x$ alloys exhibit a decreasing trend with Ag content. The lowest liquidus temperature (about 702 K) occurs at the composition of $Mg_{65}Cu_{15}Gd_{10}Ag_{10}$. In addition, the highest γ value (0.407) and a relatively high T_{rg} (0.58) occur at the $Mg_{65}Cu_{22.5}Gd_{10}Ag_{2.5}$ composition. Comparison with the γ value and T_{rg} of $Mg_{65}Cu_{25}Gd_{10}$ alloy (0.55 and 0.404) suggests that the $Mg_{65}Cu_{22.5}Gd_{10}Ag_{2.5}$ alloy would retain a high glass forming ability.

(2) The activation energy for crystallization of these $Mg_{65}Cu_{25-x}Gd_{10}Ag_x$ alloys increases with Ag content and reaches the maximum (183 kJ/mol) at the $Mg_{65}Cu_{17.5}Gd_{10}Ag_{7.5}$. This indicates that addition of Ag improves the thermal stability for the $Mg_{65}Cu_{25}Gd_{10}$ base alloy.

(3) The average value of the Avrami exponent n was 2.3 ± 0.2 for $Mg_{65}Cu_{22.5}Gd_{10}Ag_{2.5}$ alloy. This indicates that $Mg_{65}Cu_{22.5}Gd_{10}Ag_{2.5}$ alloy presents a crystallization process with decreasing nucleation rate.

Acknowledgement

The authors would like to gratefully acknowledge the sponsorship from the National Science Council of R.O.C. under the projects NSC93-2216-E-214-002, and NSC94-2218-E-110-009.

References

[1] A.A. Lou, J. Met. 54 (2) (2002) 42.
[2] M.O. Pekguleryuz, H. Kaplan, R. Neelameggham, J. Hryn, B. Powell, G. Cole, J.F. Nie, J. Met. 54 (8) (2002) 18.
[3] D.L. Albright, F. Bergeron, R. Neelameggham, A.A. Luo, H. Kaplan, M.O. Pekguleryuz, J. Met. 54 (8) (2002) 22.
[4] A. Inoue, A. Kato, T. Zhang, S.G. Kim, T. Masumoto, Mater. Trans. JIM 32 (1991) 609.
[5] A. Inoue, T. Nakamura, N. Nishiyama, T. Masumoto, Mater. Trans. JIM 33 (1992) 937.
[6] E.S. Park, H.G. Kang, W.T. Kim, D.H. Kim, J. Non-Cryst. Solids 279 (2001) 154.
[7] H. Men, Z.Q. Hu, J. Xu, Scripta Mater. 46 (2002) 699.
[8] K. Amiya, A. Inoue, Mater. Trans. JIM 41 (2000) 1460.
[9] K. Amiya, A. Inoue, Mater. Trans. 42 (2001) 543.
[10] H. Men, W.T. Kim, D.H. Kim, J. Non-Cryst. Solids 337 (2004) 29.
[11] A. Inou, K. Ohtera, K. Kita, T. Masumoto, Jpn. J. Appl. Phys. 27 (1988) 2248.
[12] K. Amiya, A. Inoue, Mater. Trans. JIM 41 (2000) 1460.
[13] G. Yuan, T. Zhang, A. Inoue, Mater. Trans. 44 (2000) 1460.
[14] C.J. Smithells, E.A. Brandes, Metals Reference Book, 5th ed., Butterworths, London, 1976, p. 100.
[15] D. Turnbull, Contemp. Phys. 10 (1969) 473.
[16] Z.P. Lu, C.T. Liu, Acta Metall. 50 (2002) 3501.
[17] H.E. Kissinger, Analyst. Chem. 29 (1957) 1702.
[18] J.W. Christian, The Theory of Transformations in Metals an Alloys, 2nd ed., Pergamon Press Inc, New York, NY, 1975.